minerals

MDPI

Article

Mineralogy, Geochemistry and Genesis of Zeolites in Cenozoic Pyroclastic Flows from the Asuni Area (Central Sardinia, Italy)

Angela Mormone * and Monica Piochi

Istituto Nazionale di Geofisica e Vulcanologia, Osservatorio Vesuviano, Via Diocleziano 328, 80124 Napoli, Italy; monica.piochi@ingv.it

* Correspondence: angela.mormone@ingv.it; Tel.: +39-081-6108528

Received: 23 December 2019; Accepted: 14 March 2020; Published: 16 March 2020

Abstract: Natural zeolite occurrences have been recognized in several Cenozoic pyroclastic deposits in central Sardinia. This study concerns the mineralogical and geochemical characterization of the zeolitized tuffites in the Asuni area (Oristano province) and aims to complement information regarding the zeolitization processes developed in the nearby Allai deposits. Optical and scanning electron microscopy, X-ray powder diffraction, qualitative vs. quantitative microanalyses and bulk-rock geochemistry were performed. Analytical results allow defining the mineral distribution, textural relationships and geochemical features of the zeolite-bearing rocks. The most abundant secondary minerals are Ca-Na mordenites. Contrarily to the most common worldwide clinoptilolite + mordenite paragenesis, mordenite is dominant and occurs in different morphologies, rarely coexisting with clinoptilolite in the studied volcanic tuffites. Glauconite and dioctahedral smectite complete the authigenic assemblages. The primary volcanic components mostly include plagioclase, quartz and glass shards, roughly retaining their original appearance. The tuffites range in composition from dacite to rhyolite. The collected dataset shows that zeolitization is most abundant in coarser-grained deposits and points to a genetic process that mainly involves an open hydrothermal environment governed by aqueous fluids with significant marine component, in post eruption conditions.

Keywords: central Sardinia; tuffites; high-silica zeolites; Mordenite; open-hydrothermal system

1. Introduction

Sardinia has been a very important mining region of the Mediterranean area with a large variety of metalliferous deposits, among which the Pb-Ag-Zn (Ba-F) ores were the most important exploited resources in the past centuries [1–4]. In more recent times, the general overview of the mining industry on the island has changed profoundly, with the closure of the Pb-Ag-Zn districts and the focus on industrial minerals (i.e., feldspars, silica sands, granites, marbles, etc.) [5–10], gold-bearing ores (Cenozoic porphyry/epithermal Au-Cu-Te and Au-Ag, and Paleozoic mesothermal "orogenic" Au deposits [11], albitite belt (central Sardinia [12]) and zeolite minerals deposits [9,13].

Natural zeolites have a peculiar framework structure characterized by channels and cages among the oxygen atoms linking the constituting SiO_4 and AlO_4 tetrahedra. These cavities have molecular-sizes and are usually occupied by H_2O molecules and extra-framework cations [14], resulting in selective properties for circulating substances on dimensional and charge basis.

Zeolitic minerals, due to the above characteristic structure, are of great industrial interest for their well-known use in several application fields [15], such as filtering [16], chemical sieve [17], odor removal [18], water softening and gas absorption [19], in cement and brick production [20], in agriculture [21], and in medicinal purposes (i.e., gastroenterology [22]).

The literature [13,23–30] provides mineralogy and areal distribution of zeolitized deposits in Sardinia and the processes of zeolitization as well. The high-silica zeolites detected in the volcano-sedimentary Oligo–Miocene successions of central Sardinia [9,26,27,30,31] should be considered potential natural resources.

Here, we focus on the Asuni area, central Sardinia, in order to (1) complete the mineralogical characterization of zeolitized deposits in the province of Oristano, i.e., those developed in the nearby Allai area [30]; (2) propose a possible scenario involving the zeolitization process and (3) give a background for potential exploitation of natural zeolites at a regional scale.

Despite the investigations carried out on Anglona [6,26,32], Logudoro-Goceano [13,23,25,28,33–35], Planargia [23], Sarcidana-Marmilla, Nureci-Fordongianus [25–27,32,36,37] and Allai areas [30], little is known about the mineralogical features and the zeolitization genetic process of the epiclastic deposits in the Asuni Unit.

Hence, we have investigated the Asuni zeolite-rich deposits by optical and scanning electron microscopy with energy dispersive spectrometry, X-ray powder diffraction, and bulk-rock geochemistry. We present the mineralogical results of zeolite-bearing rocks as well as their petrographic and geochemical features, with the final aim of describing the textural relationships of the main zeolite types throughout the epiclastic deposits and discussing the minerogenetic models.

2. Geological Background

The island of Sardinia (Figure 1) records a long geological history with a Paleozoic basement widespread from SW to NE, dissected from the later rifting phases and the magmatism [38–40]. The transtensive-extensional regime followed Eocene–Early Oligocene Alpine compressive phases and caused faulting and rifting thus leading to: (i) formation of the Oligo–Miocene rift system crossing the whole island from North to South and (ii) translation southwards and counterclockwise rotation of the Sardinia-Corsica continental microplate, with coeval opening of the Balearic back-arc basin [41,42]. Based on Cherchi et al. [43] the latest Oligocene (Chattian–Aquitanian) time corresponds to a rapid deepening of the Oligo–Miocene graben. The authors showed that during the rifting stage (Aquitanian, late Miocene), a deep marine trough already existed along the graben system axis, except in areas where the volcanism was particularly important such as in central Sardinia.

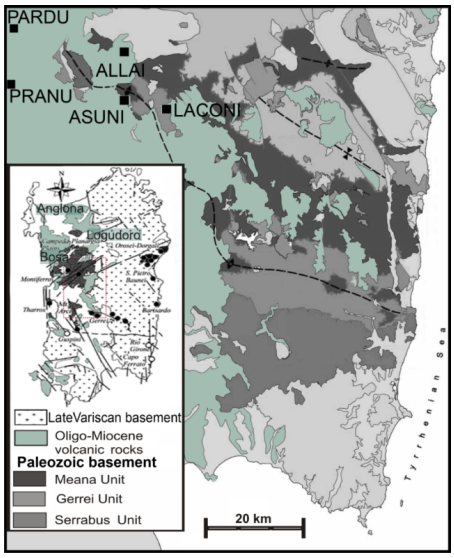

Figure 1. Simplified geological map of Central-Western Sardinia (modified by [44]), showing the outcrop area of the Oligo–Miocene volcano-sedimentary succession and the studied sites. In the area, the older Variscan basement corresponds with the Nappe Zone that consists of marine silico-clastic successions equilibrated under greenish facies. Sampled sites and labels used hereafter: P, E and I for Pranu; M and N for Asuni; H and F for Pardu.

Volcanism occurred during Oligocene–Miocene (32 to 13 Ma) and Plio–Pleistocene (5 to 12 Ma) times with different petrographic and geochemical features of produced, mostly ignimbritic, rocks [39,45,46]. The Oligo–Miocene volcanism essentially includes acid "andesitic" pyroclastic deposits and characterizes for plateau-distributed ignimbritic formations, with minor effusive rocks and epiclastic units.

The Asuni Unit is a dominant epiclastic formation of this period. It belongs to a major volcano-clastic succession of the eastern Sardinian Rift (Fordongianus–Nureci area, central Sardinia). This volcano-sedimentary succession up to ca. 300 m [47,48] includes five pyroclastic ignimbrites. Two of them are rhyolite-rhyodacite ignimbrites of the Luzzana and Allai units, both related to highly explosive phreatomagmatic episodes. These units are lowermost in the succession, overlaid by the sedimentary episclastic terrigenous-tuffaceous complex, and, in turn, by dacite lava domes and flows. The Ruinas Unit, a poorly consolidated to welded dacite ignimbrite, up to 40m thick, starts the sedimentary succession and is buried by the Asuni Unit. This latter Unit, about 50 m thick, consists of poorly welded epiclastites with composition ranging from rhyolite to dacite. It is overlain by an epiclastic arenaceous sequence formed by erosion of previous volcaniclastic formations. The latest pyroclastic products in the area form the Monte Irone Unit, a welded dacitic ignimbrite, ca.10–20 m thick.

The rhyolitic to dacitic volcanoclastic deposits often show evidence of zeolization and welding. However, studies about zeolites in the deposits from central Sardinia, are scarce [26,27,30]. In the Allai deposits, the neoformed zeolites have been related to specific physicochemical conditions (water content, temperature) of fluids circulating in the pyroclastic flows during and just after its emplacement [30]. More information exists for zeolites in the northern Sardinia. For example, in the Logudoro region zeolitization is due to circulation of hydrothermal fluids favored by the fault systems of the area [28]. In the Anglona district, fluids were either percolating groundwaters or trapped volcanic water-gas mixtures [49]. The Bosa region was affected by syn- and post- depositional zeolitization due to the phreatomagmatic fluid components [26,50].

3. Materials and Methods

Our studies were conducted on a total of 25 samples, representative of the epiclastic deposits of the Asuni Unit, found between the villages of Allai and Laconi (Figure 1).

The investigated sequences were sampled at different stratigraphic heights in seven outcrop sites (labelled H, F, P, I, E, N, and M in Figure 2), albeit stratigraphic correlation was impossible due to the absence of interbedded paleosols or discontinuities, and recognized marker levels. Sampling was based on different sedimentological and lithological appearances, in order to investigate the possible relationships between the primary volcanological features and the secondary mineral assemblages.

The samples were ground to ca. 5 mm and divided in two halves, similar for texture and lithology. The first half was used to prepare polished sections and stub-positioned portions for optical microscopy (OM), electron microscopy and microanalysis; the second one was pulverized for X-ray diffraction and whole-rock geochemistry.

X-Ray powder diffraction (XRPD) made use of a Panalytical X'Pert PRO PW 3040/60 diffractometer equipped with a pyrolitic graphite analyzer crystal at the "Istituto per i Polimeri, Compositi e Biomateriali", Centro Nazionale delle Ricerche, Pozzuoli, Italy. We used unfiltered CuKα radiation in the following conditions: accelerating voltage 40 kV, tube current 40 mA, 3°–70° 2θ range, steps of 0.02° 2θ, counting time in 30 s/step, 0.5 mm divergence slit, 0.1 mm receiving slit, and a 0.5° anti-scatter slit. Few samples were analyzed at the Dipartimento di Scienze della Terra, dell'Ambiente e delle Risorse (DiSTAR) University of Naples Federico II (Napoli, Italy). In this case, we used a Seifert–GE ID3003 diffractometer (Napoli, Italy), with CuKα radiation, Ni-filtered at 40 kV and 30 mA, in the 3–70° 2θ range, a 0.02° 2θ step scan, time of 10 s/step and the RayfleX (GE) software package (Inspection Technologies, 2004). All powdered samples were side-loaded to minimize eventual

preferred orientation effects. The qualitative identifications were carried out through the search–match software and the ICDD PDF2 database (version 2012, Napoli, Italy).

Optical microscopy (OM) on thin sections was performed using a Leica DFC280 microscope (Leica, Wetzlar, Germany) to observe the textural features and the petrographic composition of samples.

A JEOL JSM 5310 scanning electron microscopy (SEM) integrated with an energy dispersion spectrometry (EDS) operating at Dipartimento di Scienze della Terra, dell'Ambiente e delle Risorse, DiSTAR, University of Naples Federico II (Napoli, Italy), was used for micro-morphological and chemical study both on fragments and polished thin sections. Fragments were fixed onto aluminum stubs with double-stick carbon tape, whereas thin sections were positioned on aluminum planar holder after coating by carbon about 10 nm thick under a vacuum evaporator, observed by SEM and analyzed by EDS. The following conditions were adopted: 15 kV electric current, 50–100 µA filament current, variable spot size and 20 mm working distance. EDS based an automated qualitative elemental analysis mode by Oxford (INCA) with ZAF matrix correction, using standards of anorthoclase for Si, Al and Na, diopside for Ca microcline for K, rutile for Ti, fayalite for Fe, olivine for Mg, serandite for Mn, sphalerite for Zn. Detection limits of the analyzed elements are below 0.1%.

Whole-rock geochemistry was carried out at Bureau Veritas Commodities Canada Ltd. (Vancouver, Canada). Major elements were determined on dried sample powders mixed with lithium tetraborate/metaborate flux followed by fusion and casting into glass discs, by X-ray fluorescence (XRF; method XF701). Minor elements were determined by inductively coupled plasma-mass spectrometry (ICP-MS) after $LiBO_2/Li_2B_4O_7$ fusion of powdered sample (method LF100; Bureau Veritas Commodities Canada Ltd., Vancouver, Canada). Moisture and loss on ignition (LOI) were determined separately at 105 °C and 1000 °C.

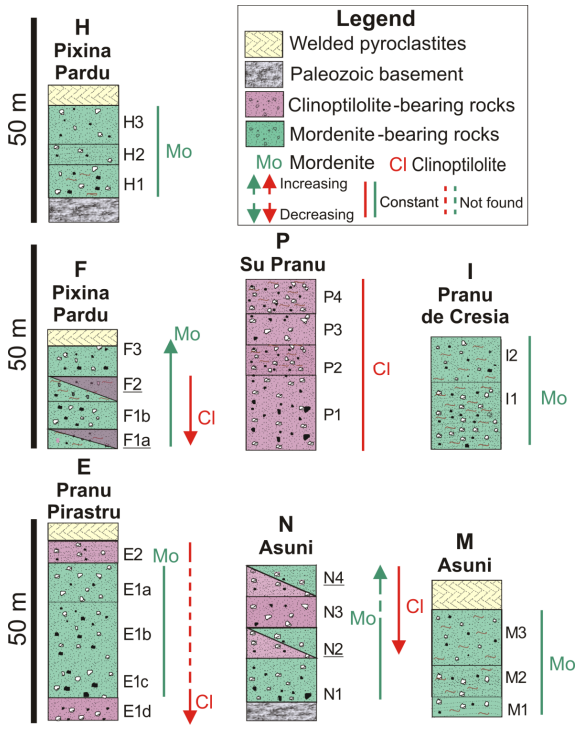

Figure 2. Sketch of sampled stratigraphic sections at the sites in Figure 1, arranged from North-West to South-East and completed by qualitative abundance of secondary minerals. Underlined sample names highlight clinoptilolite and mordenite coexistence. In the legend, the deposits are distinguished based on dominant zeolite. Note: The relative abundance in collected samples allows to infer the vertical trend in the zeolite stratigraphy.

4. Results

4.1. Sedimentological, Petrographic and Mineralogical Descriptions

The sampled sequences of the Asuni Unit are mostly epiclastic tuffites, with an extensive brown-yellowish appearance (Figures 3a,c and 4) and a cohesive to hard consistency (Figure 4a,c). The sequences consist of a series of coarse sandy-to-ashy layers with variable thickness of down to ca. few centimeters, showing planar-to-medium angle lamination and locally characterized by greenish (most common) and blackish or reddish (occasional) tones (Figures 3c and 4c). Coarse (grain size up to dm) dense fragments are widespread in the deposits with an abundance between 25 vol % (upper portion) and 40 vol % (lower portion); the denser blocks are highly to poorly welded ignimbrites, andesite lavas and Paleozoic crystalline basement rocks. Pumices occur in low amounts. They are usually broken and represented by brown to white and light gray colors; elongated vesicles often aligned to a tube structure are also observed. Overall, pumices are coarser in the uppermost levels with size of 1 to 5 mm in diameter. Based on bulk-rock geochemistry of selected samples, the Asuni tuffites are dacites, rhyodacites to rhyolite (Tables 1 and 2).

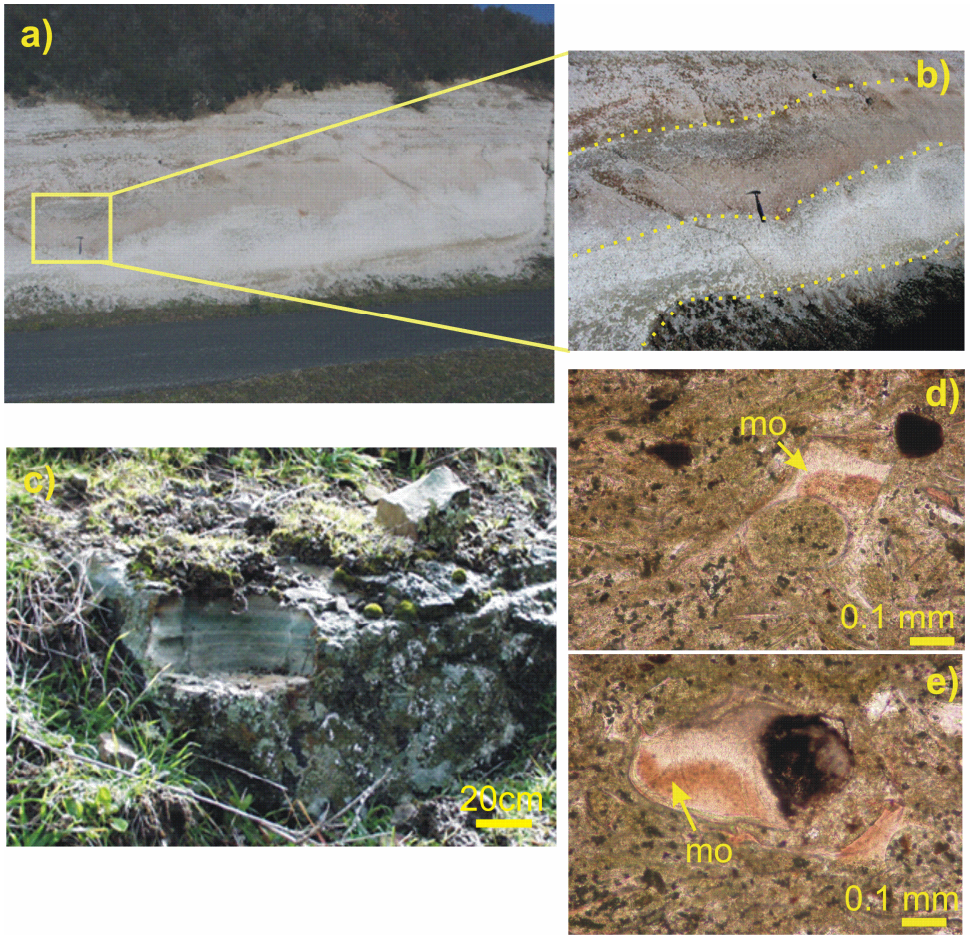

Figure 3. The Asuni Unit: (**a**,**b**) interbedded whitish and laminar ashy-to-sandy deposits (F sequence in Figure 2); (**c**) typical outcrop showing greenish layering (I sequence in Figure 2); (**d**,**e**) photomicrographs obtained under plane-polarized transmitted light showing the altered ashy-to-sandy matrix and widespread mordenite.

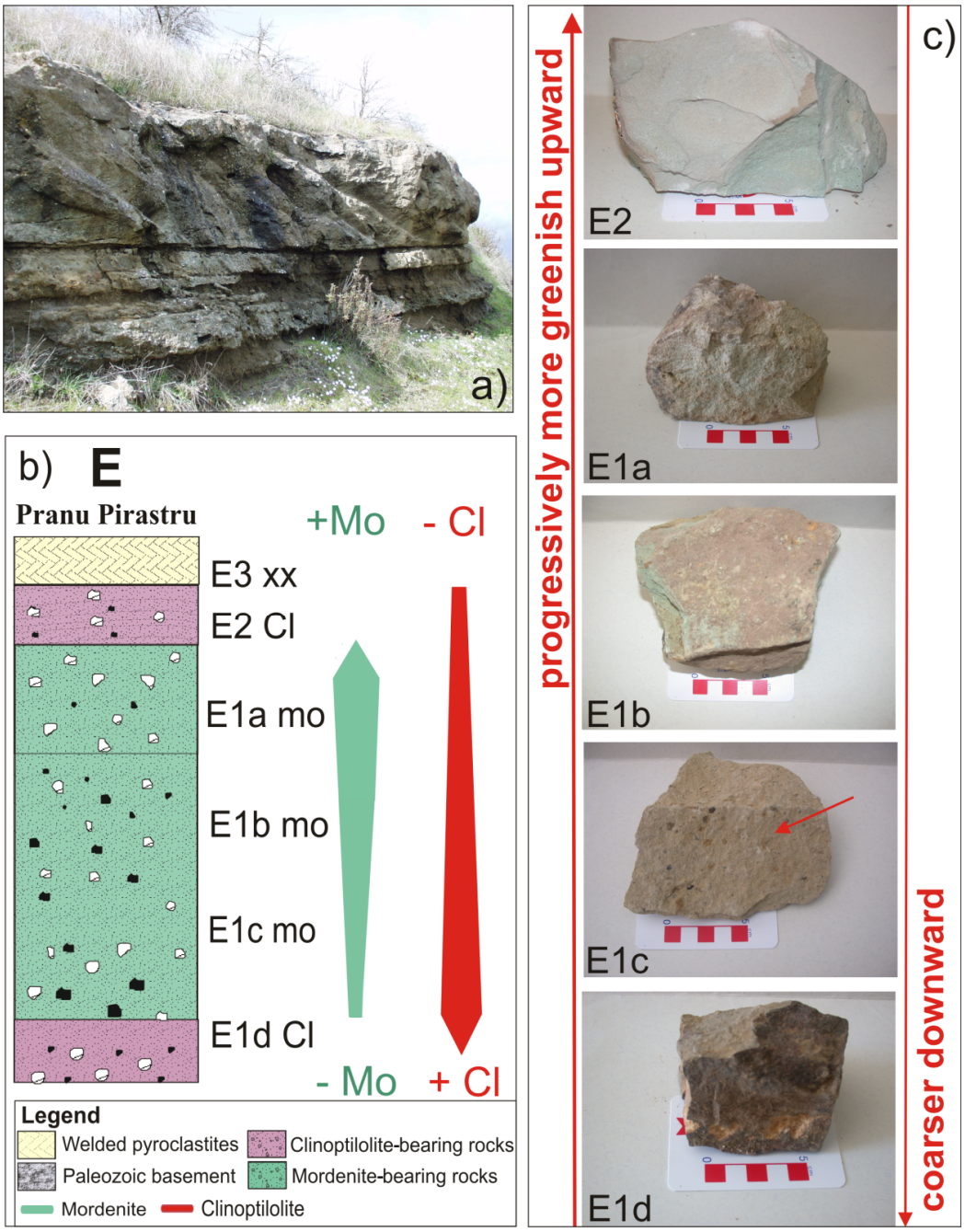

Figure 4. The Asuni unit at Pranu Pirastru (Pranu in Figure 1). (**a**) Representative laminated outcrop deposit; (**b**) reconstructed "E" lithostratigraphic sequence and relative zeolites vertical distribution; (**c**) photos of selected samples arranged base-upward to show the vertical textural change. The scale bar is 5 cm. See Supplementary Materials Figure S1 for XRPD patterns of the zeolite-bearing samples.

Table 1. Summary of mineralogical and petrographic features of the studied Asuni samples.

Sample	Locality	Petrographic Type	Phenocrysts	Secondary Mineralogy
	Pardu			
H1	Pixina Pardu	Rhyodacite	pl, K-fd, qz, bt	Sm, mo
H2	Pixina Pardu	Rhyodacite	pl, K-fd, qz, bt	Sm, mo
H3	Pixina Pardu	Rhyodacite	pl, K-fd, qz, bt	Sm, mo
F3	Pixina Pardu	Rhyodacite	pl, K-fd, qz, bt, hem	Sm, mo
F2	Pixina Pardu	Rhyodacite	pl, qz, K-fd, bt, hem	Sm, cl, mo
F1b	Pixina Pardu	Rhyodacite	pl, K-fd, qz, bt, hem	Cl, sm
F1a	Pixina Pardu	Rhyodacite	pl, qz, bt, hem	Cl, sm, mo
	Pranu			
E2	Pranu Pirastru	Rhyolite	pl, K-fd, qz, bt	Sm, cl
E1a	Pranu Pirastru	Rhyolite	pl, K-fd, qz, bt	Sm, mo
E1b	Pranu Pirastru	Rhyolite	pl, K-fd, qz, bt	Sm, mo
E1c	Pranu Pirastru	Rhyolite	pl, K-fd, qz, bt	Sm, mo
E1d	Pranu Pirastru	Rhyolite	pl, K-fd, qz, bt	Sm, cl
I2	Pranu de Cresia	Rhyodacite-dacite	pl, K-fd, qz, bt, hem	Sm, mo
I1	Pranu de Cresia	Rhyodacite-dacite	pl, K-fd, qz, bt, hem	Sm, mo
P4	Su Pranu	Rhyolite	pl, K-fd, qz, bt, hem	Sm, cl
P3	Su Pranu	Rhyolite	pl, K-fd, qz, bt, hem	Sm, cl
P2	Su Pranu	Rhyolite	pl, K-fd, qz, bt, hem	Sm, cl
P1	Su Pranu	Rhyolite	pl, K-fd, qz, bt, hem	Sm, cl
	Asuni			
M3	Asuni	Rhyodacite	pl, K-fd, qz, hem	Sm, mo
M2	Asuni	Rhyodacite	pl, K-fd, qz, hem	Sm, mo
M1	Asuni	Rhyodacite	pl, K-fd, qz, hem	-
N4	Asuni	Rhyolite	pl, K-fd, qz, bt, px, mt	Sm, cl, mo
N3	Asuni	Rhyolite	pl, K-fd, qz, bt, px, mt	Sm, cl
N2	Asuni	Rhyolite	pl, K-fd, qz, bt, px, mt	Sm, cl, mo
N1	Asuni	Rhyolite	pl, K-fd, qz, bt, px	Sm, mo

Abbreviations: pl: plagioclase, K-fd: K-feldspar, qz: quartz, bt: biotite, px: pyroxene, mt: magnetite, hem: hematite, cl: clinoptilolite, mo: mordenite, sm: smectite, based on XRPD analyses, corroborated by EDS-SEM investigations.

Table 2. Major (wt. %) and minor (ppm) elements concentration of studied samples, obtained by means of ICP analysis.

Oxide wt %	E1a	E1b	E1d	E2
SiO_2	67.98	64.53	70.92	67.27
Al_2O_3	12.84	13.06	10.30	11.66
Fe_2O_3	1.54	2.47	3.48	1.97
MgO	0.36	0.76	0.79	0.97
CaO	1.65	2.34	1.64	2.82
Na_2O	1.16	2.04	0.67	0.93
K_2O	6.50	3.51	3.15	2.91
TiO_2	0.40	0.39	0.38	0.39
P_2O_5	0.05	0.03	0.07	0.11
MnO	0.04	0.04	0.02	0.02
LOI	7.40	10.90	8.40	10.90
Tot	99.98	100.01	99.78	99.95

Table 2. *Cont.*

Oxide wt %	E1a	E1b	E1d	E2
		Element in ppm		
Ba	714.00	367.00	519.00	827.00
Be	1.00	2.00	2.00	2.00
Co	1.40	1.10	2.60	2.80
Cs	2.90	4.10	2.30	1.50
Ga	11.90	12.40	11.40	11.20
Hf	6.60	6.40	5.00	6.00
Nb	12.10	12.10	9.40	11.70
Rb	109.40	111.00	71.60	62.70
Sn	2.00	2.00	1.00	2.00
Sr	197.90	216.30	286.80	592.60
Ta	0.80	0.80	0.60	0.70
Th	10.20	11.10	9.70	10.40
U	2.40	2.40	3.40	2.30
V	14.00	16.00	29.00	15.00
W	0.80	0.60	0.80	0.50
Zr	209.40	196.50	143.50	183.50
Y	32.90	26.00	26.10	45.90
La	28.00	30.70	26.30	29.90
Ce	57.80	48.50	49.50	58.90
Pr	7.82	7.72	6.50	8.39
Nd	27.20	26.90	26.10	32.20
Sm	5.53	4.78	4.72	6.42
Eu	1.02	1.04	0.90	1.19
Gd	4.44	4.01	4.07	6.64
Tb	0.86	0.77	0.72	1.11
Dy	5.20	4.73	4.16	6.56
Ho	1.20	1.05	0.98	1.43
Er	3.43	2.80	2.54	3.80
Tm	0.59	0.48	0.46	0.63
Yb	3.52	2.66	2.62	3.77
Lu	0.61	0.44	0.47	0.70
Mo	0.10	<0.1	1.40	0.30
Cu	5.00	3.70	15.90	12.50
Pb	10.40	7.10	16.60	14.20
Zn	38.00	25.00	44.00	49.00
Ni	0.50	0.40	3.00	0.40
As	<0.5	0.80	27.00	8.40
Cd	<0.1	<0.1	0.30	0.40
Sb	<0.1	<0.1	0.30	<0.1
Bi	<0.1	<0.1	0.10	<0.1
Ag	<0.1	<0.1	<0.1	<0.1
Au *	7.80	12.70	7.80	44.90
Hg	0.02	0.01	0.02	0.03
Tl	<0.1	0.10	1.40	0.20
Se	<0.5	<0.5	0.70	<0.5

Note: * ppb.

Under the optical microscope, the samples show variable textures and colors, even though they share common features. Their primary crystalline component is represented by fractured and altered plagioclase grains (Figure 5a,b), alkali-felspars, rounded quartz (Figure 5c) and altered biotite laths (Figure 5d). Rare pyroxene and accessory apatite, hematite and/or magnetite crystals are also recognized. The glassy component is widespread, forming the bulk matrix and the cuspidate shards (Figure 5d,f, and Figure 6a,b). Moreover, the dark brown, greenish and reddish colors of the bulk matrix can be seen, together with other evidence of post-depositional and alteration processes, i.e., (1) zeolite

and minor clay minerals growing in the rock cavities (i.e., vesicles, voids, fractures), on the crystals and/or at the expense of glassy component (Figure 5f); (2) pervasive greenish formations running for few mm across the bulk-matrix (Figure 5e) or thinly coating the glass component (Figures 5f and 6f); (3) rock fractures filled by greenish and whitish mineralization (Figure 5g,h); (4) dissolution areas in quartz (Figure 5c). We attribute the above green aggregates within the veins and widespread in the bulk matrix of the samples to glauconite, as constrained by microanalyses performed on well crystallized minerals within fracture (Figure 5g,h). Voids can host small k-feldspar and quartz that coexist with the dominant zeolites and cannot be considered primary but are later secondary phases.

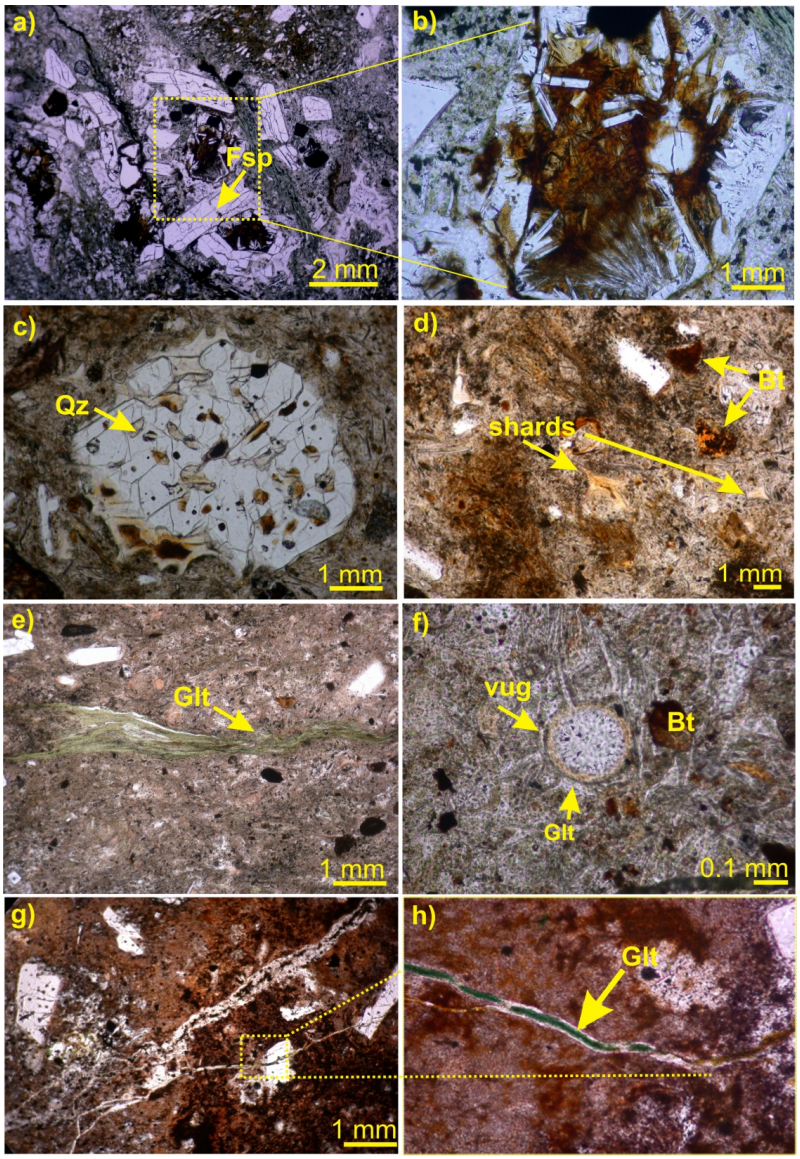

Figure 5. Microphotographs showing textural and mineralogical features of selected samples under OM: (**a**,**b**) Feldspar with alteration signs in I1 sample under plane polarized light; (**c**) rounded quartz with several micro-voids in H2 sample, under cross polarized light; (**d**) cuspate glassy y-shaped shards partially transformed into clinoptilolite aggregate in the H3 altered epiclastites under cross polarized light; (**e**) glauconite in ashy sample E1a, under plane polarized light; (**f**) vugs filled by clinoptilolite crystals in E2 sample, under plane polarized light; (**g**) glauconite and (**h**) its particular grown in veins crossing the reddish matrix of the sample E1d, under plane polarized light. Note the vein-filling or fluid-miming aspect of glauconite mineralization in (**e**,**h**). Abbreviations: Fsp: feldspar; Qz: quartz; Glt: glauconite; Bt: biotite.

Table 1 reports the mineralogical composition of both primary and secondary minerals derived by combined XRPD analyses and OM-SEM observations.

Primary minerals, i.e., plagioclase and quartz, amounts are prevailing phases, associated with a ubiquitous amorphous fraction.

Zeolites are the most important and widespread secondary ore minerals, and are mainly represented by mordenite and subordinate clinoptilolite (Table 1, Figures 2 and 6).

Zeolite abundance seems to depend on the glass matrix availability. Mordenite forms mostly acicular crystals growing at the expense of the glass components such as shards, cineritic matrix and/or spherical cavities (Figure 6d–f). Despite the low content, euhedral tabular clinoptilolite crystals fill the spherical cavity where they grew upwards (Figure 6a), deeply transforming the cuspate glass shards (Figure 6b) and locally replacing the glassy matrix (Figure 6c). Tabular clinoptilolite can coexist with acicular mordenite, particularly in vugs of coarser aggregates (Figure 6a). In association with clinoptilolite plats, mordenite appears to determine spherulitic aggregates (Figure 6a) and is likely a later phase. Clay minerals are subordinate [26].

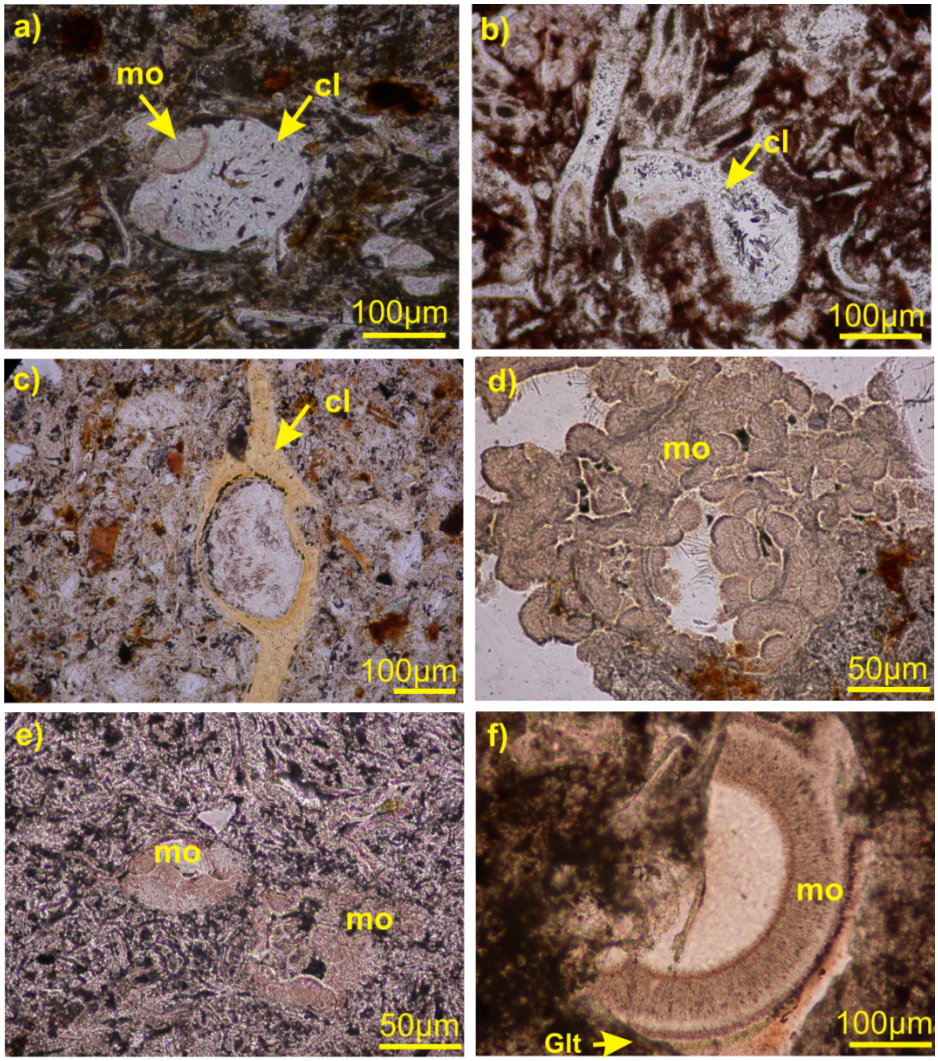

Figure 6. Microphotographs of zeolites in samples observed under a plane-polarized transmitted light: (**a**) armored lapilli altered into clinoptilolite aggregate and spherulitic mordenite, sample N2; (**b**) felt-shaped aggregates made up of well-developed clinoptilolite crystals, sample N3; (**c**) voids in the glassy-shards bearing tuff matrix filled by euhedral crystals of clinoptilolite, sample P1; (**d**) glassy component transformed by acicular mordenite, sample E1b; (**e**) sub-spherical vesicle disperse in the tuff matrix containing radiating mordenite crystals, sample H2; (**f**) detail of radial mordenite, sample H1.

Figure 2 shows the seven Oligo–Miocene volcanic sequences and the distribution of zeolites.

The occurrence of mordenite and clinoptilolite is variable, both among sequences and inside along a single outcrop. On the basis of the OM and XRPD we observe that (i) the strongly cohesive ignimbrites are unzeolitized; (ii) mordenite is the most abundant zeolite and increases towards the high stratigraphic levels (i.e., sequences N, F, E, M); (iii) clinoptilolite seems to increase proceeding downwards (i.e., sequence N, F); (iv) H and I sequences are characterized by mordenite only; (v) dioctahedral smectite is ubiquitous, but its content is low (see Cappelletti et al. [26]). However, an inverse correlation between the clinoptilolite and mordenite may be observed. Furthermore, the relation is positive considering coarse-grained layers where the authigenic phases are more abundant.

4.2. SEM Observations and EDS Microanalysis

Dioctahedral smectite occurs as thin plates along the outer side of the glass shards and precedes the zeolite crystallization, as assumed by textural relationships.

Mordenite displays three main morphologies that coexist in the same sample and, based on observations, we confidently associate with the alteration stage.

The first mordenite type consists of tiny crystals emerging from the glassy component and/or from its substratum smectite coating (Figure 7a). This mordenite can represent an embryonic stage of zeolite growth; it produces limited replacement of the glass phase that still shows the proper primary or early argillification features. The second mordenite type is a stubby fibrous microcrystals that assembly in characteristic "inter-twinned bundles" (Figure 7b,c). In this occurrence, mordenite is finely intergrown with smectite, crystallizing at the expense of the clay mineral (Figure 7d). Figure 7b–d displays this second morphological type within vugs of both the pumice and host matrix. The mordenite is rarely covered by plate-like smectite (Figure 7f). The third mordenite (Figure 7g) arranges in tuft and occurs on euhedral clinoptilolite crystals. In this latter case, mordenite has an acicular shape with slender fibers, which can reach up to 40 μm in length. Otherwise, in the first and in the second types, mordenite is very small and rarely reaches 5 μm in length.

Contrarily to mordenite, clinoptilolite always shows a well-developed crystal habit (Figure 7h,i). In coarse-grained assemblages, clinoptilolite laths reach their largest size of 30 μm along the *c* axis and thickness of ca. 5 μm, showing characteristics of monoclinic symmetry. When grown on glassy shards, clinoptilolite forms radial arrangements.

Chemical composition of the studied mordenite and clinoptilolite is in Supplementary Materials Tables S1 and S2. Plotted in a (Ca + Mg)-Na-K ternary diagram (Figure 8a,b), these zeolites display wide chemical variations. In particular, the clinoptilolites have (Mg + Ca) in the range 1.69–2.72 (atoms per formula unit, hereafter apfu), Na at 0.48–2.59 apfu, and K at 0.16–0.64 apfu; while the mordenite yielded (Mg + Ca) values of 1.53–4.01 apfu, Na of 0.84–3.77 apfu, and K of 0.28–3.33. Therein, clinoptilolite that was studied here is characterized by a lower K content and a higher Ca/K ratio with respect to mordenite (Ca/K at 0.44–8.43 vs 2.22–10.19, respectively; Figure 8b,c). Furthermore, together with mordenite, it manifests high Ca content (1.4–1.95 in clinoptilolite and 1.44–2.54 apfu in mordenite). The average chemical composition of the two zeolites portrayed their calcic character, with Si/Al ratios at 4.43–5.01 and 4.13–5.42, respectively. These values fit the theoretical estimates (Si/Al = 5 [51]), although the ratios are lower for clinoptilolite).

Mordenites and clinoptilolites measured in the Allai unit [30] and those studied here perfectly overlap in terms of building major oxides (Figure 8d) and extra framework cation contents (Figure 8a). However, when compared to literature data ([52–54] and reference therein), the Asuni zeolites are characterized by lower Na (Figure 8e,f) and higher Ca + Mg content (Figure 8a). Notably, the Mg cation of clinoptilolite is mostly at around 1apfu (Figure 8f).

Furthermore, the mordenite in sequence I (see envelop by dashed line in Figure 8e) is richest in K (i.e., ca. 3 apfu for those in shards and cavities, respectively). The mordenites occurring in sequence H exhibit a higher Na content (up to 3.77 apfu) compared to others (see envelop by dashed line in Figure 8e). However, the Na cations decrease moving upwards along the sequence (arrow in Figure 8f).

Finally, OM and EDS analyses (Figure 5g,h) show glauconite occurring in veins and often in the bulk matrix, as well as being responsible for the greenish color of the studied deposit.

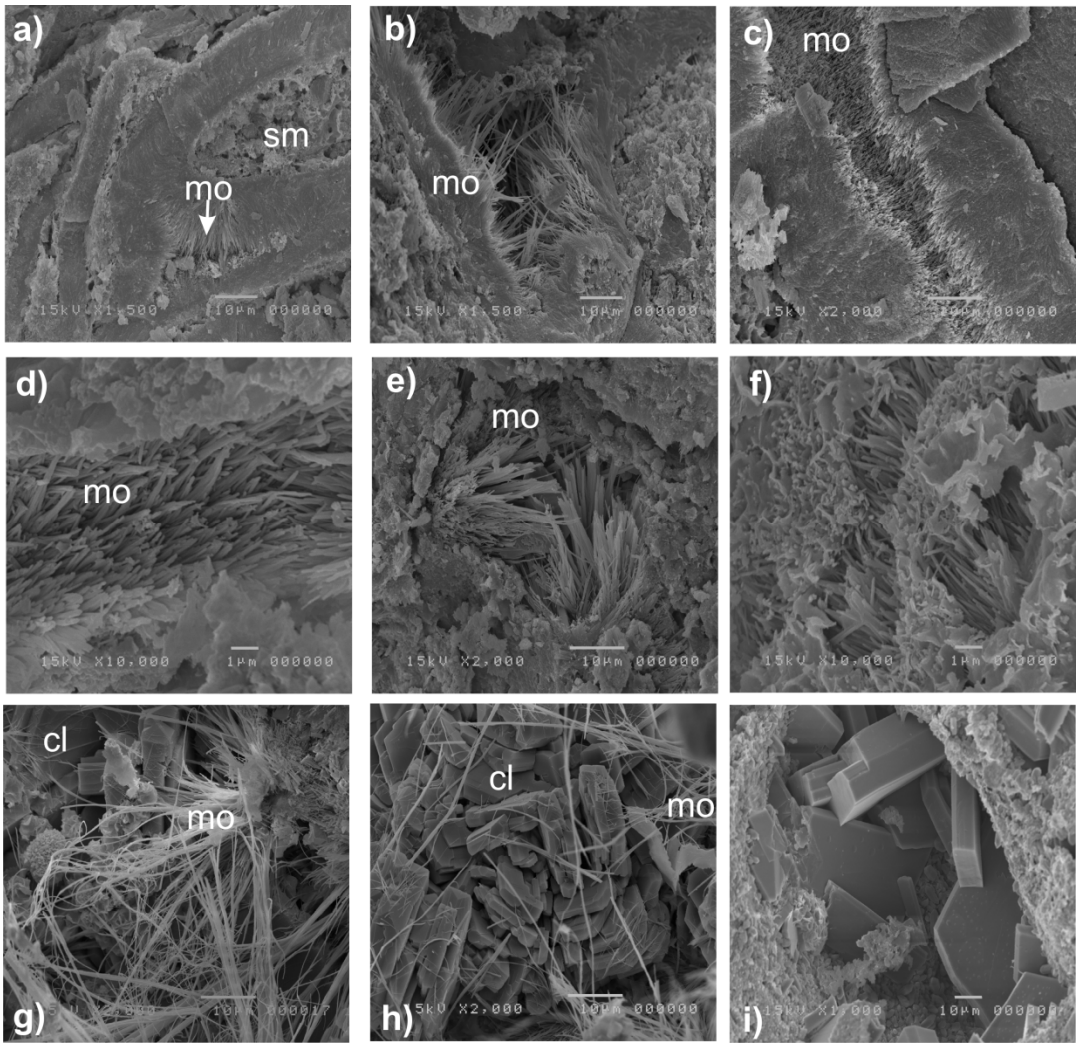

Figure 7. B-SEM (Back Scatter Electron Microscope) images of selected zeolite-bearing samples. (**a**) Incipient dissolution of the cuspate shards to mordenite in aggregating crystals, sample E1b; (**b**,**c**) from volcanic glass dissolution nucleated and growth acicular crystals of mordenite with characteristic "intertwined bundles", sample E1a; (**d**) shards altered to acicular mordenite, sample E1b; (**e**,**f**) micro-cavities filled by acicular aggregating mordenite crystals, sample E1b; (**g**) mordenite with acicular shape grown on the glassy component, sample F3; (**h**) small cavity filled by clinoptilolite laths on which rare acicular mordenites occur, sample F2; (**i**) cavity filled by euhedral clinoptilolite, F1a.

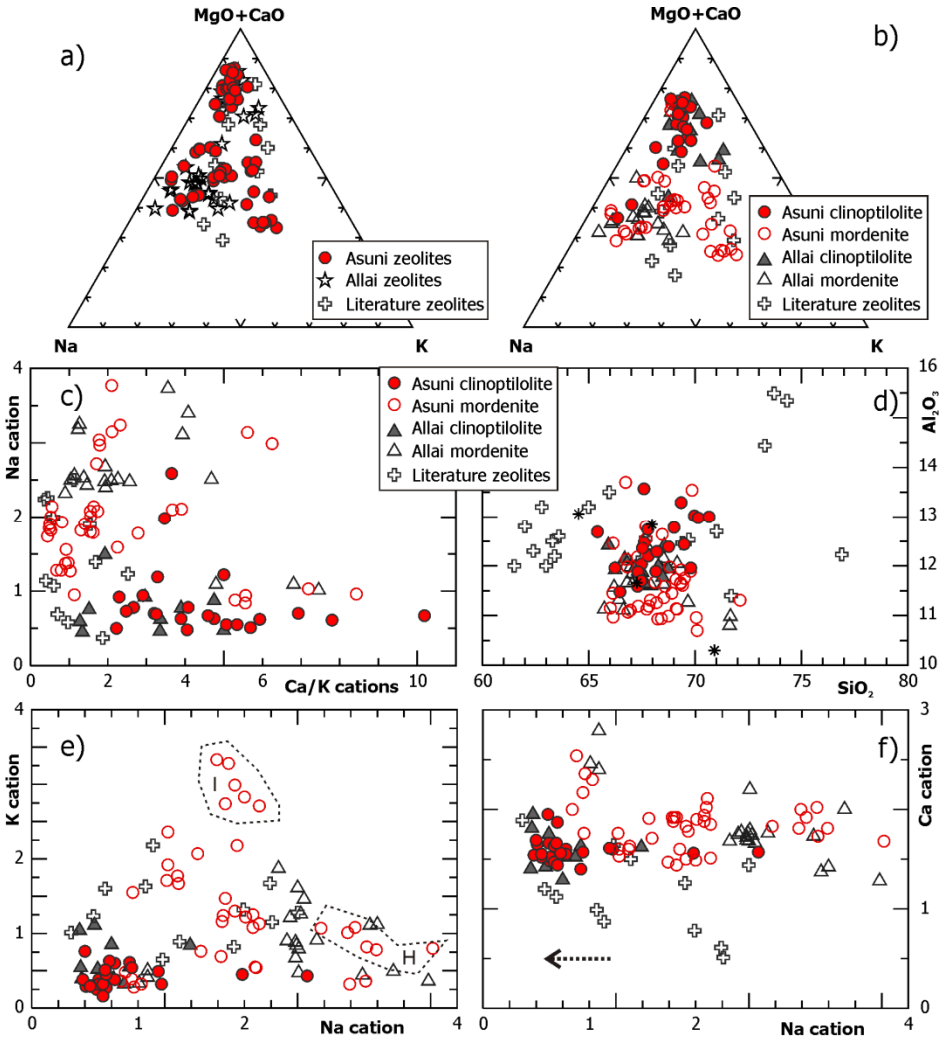

Figure 8. Zeolite composition of the Asuni samples plotted into triangular diagrams (Ca + Mg)-Na-K (**a**,**b**) and binary diagrams of measured content in cations (**c**,**e**,**f**) and oxides (**d**) and compared with literature data [25,53,55]; the arrow shows main trend along sequence. The plots allow the comparison with literature on clinoptilolite and mordenite chemistry, namely, from Allai Unit [30] and other Si-rich zeolites worldwide. Errors are within symbol size.

5. Discussion

The XRPD and EDS-SEM results indicate that the Asuni tuffites are altered but moderately zeolitized. The studied deposits contain more than half of the primary mineral components, i.e., plagioclase, quartz and K-feldspars (Table 1). It is also possible to recognize several glass shards with a broad primary structure and characteristic cuspate shapes (Figures 5d and 6b). The authigenic minerals are subordinate (as found by [26]), and mainly represented by mordenite and clinoptilolite, with subordinated smectite and glauconite (Table 2; Figures 5 and 6). Similarly to other deposits of central Sardinia [9,26,27,30,31], mordenite is the most widespread and can be the sole zeolite phase. Glauconite is instead uncommon in this area.

The Asuni Unit was deposited in a sub-aqueous environment [44,47]. More in detail, Assorgia et al. [47] indicated a lacustrine-type depositional environment for the Asuni Unit, on the basis of sedimentological and stratigraphic evidence. These authors suggest that the unit consists of fluvial-lacustrine sediments that derive from erosion, reworking and short transport of previous volcanoclastic formations. Moreover, Cherchi et al. [44] proposed a detailed Oligo–Miocene chronology of the tectonic and of the sedimentary events, also defining environment and deposition depth based

on chrono-biostratigraphical considerations. In specifying the timing of pre-, syn-, and post-rift stages in the Oligo–Miocene graben system of Sardinia, the authors dated the first marine ingression in latest Oligocene and, by further considering seismic reflection profiles, indicating a rapid subsidence and deep-water sedimentation during Oligo–Miocene in central Sardinia. There is substantial textural and mineralogical evidence corroborating these geological and paleo-environmental reconstructions.

Evidence of the sub-aqueous environment is the diffuse greenish color of the studied sequences, both in the field observations and at macro-to-microscale investigations; which also show a characteristic layered arrangement (Figures 3 and 4). OM and EDS microanalyses on thin sections (Figure 5e,g,h) show that these greenish formations contain glauconite. According to literature [56–60], glauconite growth derives from (i) alteration of the clay component through addition of Fe, (2) supply of K to the growing smectites (with glauconite- smectites transformation). The two processes are favored in K-enriched rocks and generally occur in marine or hypersaline aqueous environments. Although oversimplifying, we are confident in recommending that propose that the lacustrine environment basin, in which the Asuni tuffites are deposited, was produced by the marine ingression in the central Sardinia subject to the extensive tectonics. In these regards, Cherchi et al. [44] showed that during the rifting stage (Aquitanian, late Miocene), there was already a deep marine environment in the graben, except for the areas subject to the volcanism-derived sedimentation, like central Sardinia.

The mineralogical data obtained on zeolites provides further evidence for an active hydrothermal system and points to the circulation of fluids depending on permeability over other parameters. As a matter of fact, the type and abundance of zeolites cannot be related to differences in rock components (i.e., lithic clasts, juvenile elements, minerals) that are homogeneously distributed in all the studied Asuni sequences. The zeolite chemistry is independent from bulk-rock compositions (rhyolite, rhyodacite and dacite; Tables 1 and 2) and location (Figures 1 and 2). However, clinoptilolite and mordenite contents are higher in very coarse-grained layers compared to the other, fine-grained, levels (Figure 4b). Clinoptilolite occurs abundantly in the lowermost and intermediate levels of the stratigraphic sequences, with an apparent increase in clinoptilolite contents moving from top downwards. Contrarily, mordenite occurs more frequently in the upper layers and sometimes tends to disappear towards the bottom, particularly in successions where it coexists with clinoptilolite. The described distribution of zeolites is testified by the sequence E (Pranu Pirastru, Figure 4). Here, the very coarse-grained aggregates, which corresponds to the maximum zeolite content, as confirmed by OM and SEM investigations (in Section 4.1).

In open hydrological systems, the vertical zoning of zeolites is explained in terms of progressive chemical-physical variations of percolating solutions, leading to formation of different zeolite species [61]. This process justifies the vertical zonation of authigenic minerals in the Asuni Unit, supporting the possible formation of zeolite in an open hydrologic system, as also hypothesized by Cappelletti et al. [26]. This type of system also accounts for the cations in the analyzed zeolites that have content too high with respect to those in the bulk epiclastites and the Na trend of zeolite chemistry (Table 2; Supplementary Materials Tables S1 and S2). In addition, Asuni bulk epiclastites, if compared to those Allai and free-zeolites [62], showed an enrichment in CaO (and K_2O) and a depletion in Na_2O content (Figure 9a,b), so that three distinct fields can be suggested: Asuni, Allai and free-zeolite. We think that this distribution has a genetic significance and can offer important information to distinguish minerogenesis in various zeolitic rocks. There are few constraints to explore the Ca distribution. The experiments by Wirshing et al. [63] suggest that the kind of calcium zeolites strongly depends on the presence of an open system. In particular, products increasingly rich in calcium required a Ca-rich external reactant solution, which provided available Ca^{2+} and thus justified the formation of calcium zeolites.

Our data, therefore, corroborate the hypothesis about a major contribution from external fluids. It is also remarkable that the REE concentrations are higher in Asuni epiclastites with respect the Allai pyroclastic Unit. The Asuni patterns are shifted-upward, even if mutual fractionations among REEs

are roughly similar. Rock compositions cannot explain this difference, as the two units are similar in SiO_2, Al_2O_3 and alkali contents (Figure 9b).

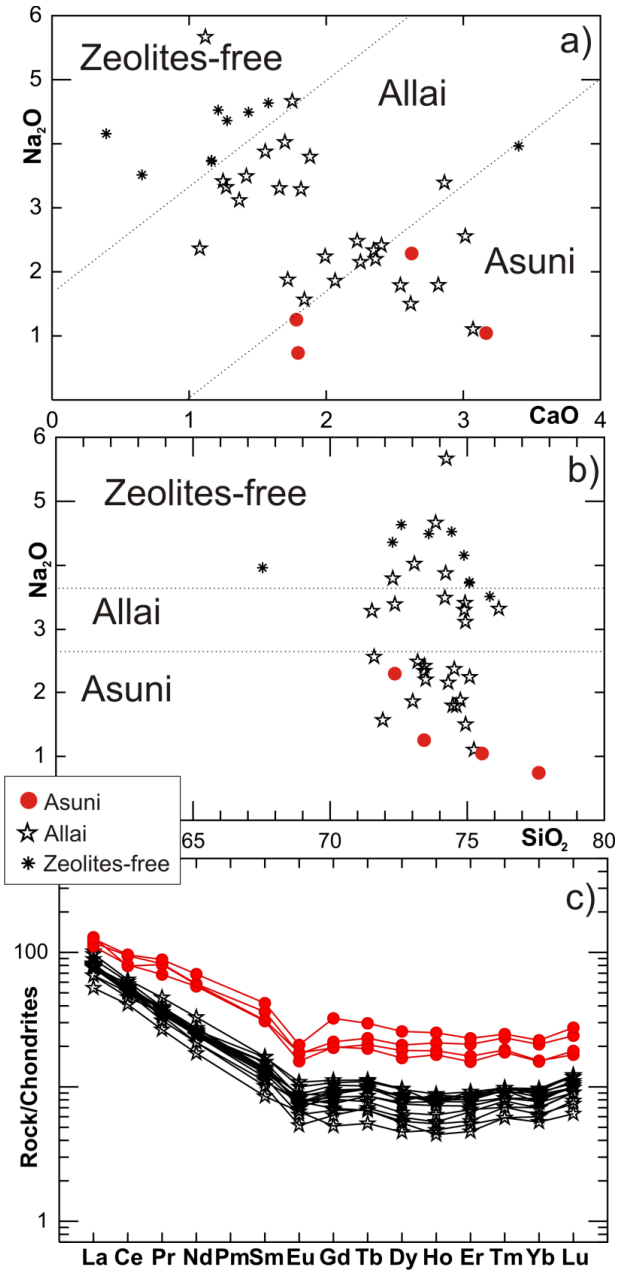

Figure 9. Plots showing the geochemistry of Asuni and Allai bulk-rocks and the related evolutionary trends: (**a**) CaO vs Na_2O and (**b**) SiO_2 vs Na_2O; the dashed line confines the Asuni and Allai zeolitized from zeolites-free rocks; (**c**) REE patterns of Asuni and Allai samples normalized to chondrites. Data from Table 2 and [30,62]. Chondrite values from [64].

However, Allai deposits tend to be rich in LREE relative to HREE, contrary to the Asuni rocks that show nearly flat patterns. In our opinion, the REE patterns and the alteration type provide evidence for the limited involvement of primary fluids in the Asuni tuffites which instead was dominant in the Allai pyroclasts. This is in agreement with the lithology of the deposits.

Additional support to the open system model comes from the textures of some zeolites, which form cement around denser and residual mineral fragments in the studied Asuni sequences (Figure 7h,i) and in other volcanic products of central Sardinia affected by a post-depositional alteration [29].

The possible zeolitization sequence for the Asuni Unit is schematized as follows:

glass ↦ smectite ↦ mordenite (I-II type) and/or clinoptilolite ↦ mordenite (III type)

This sequence of zeolite crystallization is very common in natural open system environments and is in agreement with literature data from Sardinia [28,30,34,65] and elsewhere [52]. At Asuni, it is also supported by morphology of mordenites (e.g., mordenite type in Section 4.2).

The early mordenites are first and second types (e.g., embryonic and fibrous, respectively) which originated as a direct expense of volcanic glasses under the action of alteration fluids (Figures 7 and 10). In this case, the zeolitization is peripheral to vugs and y-shards, which likely trapped original fluid at the moment of deposit emplacement. By considering previous studies [66–68], the Si and (mainly alkalies) cation contents of mordenite depends on the Si and cation contents of the glass and on the pH of the permeating solutions (being at ca. 7 in "open systems") (Figure 10a,b).

The later third mordenite type (tuft morphology) followed the clinoptilolite crystallization and/or the external supply (Figure 10c). SEM investigations show that web-like fibers of mordenite have grown both on the glassy components (i.e., Figures 6e and 7g) and between clinoptilolite crystals (Figure 7h). Clinoptilolite seems to form in response to the progressive chemical changes of fluids towards higher Ca/K ratios and perhaps the availability of Mg^{2+} cations of marine water origin. It rarely forms crystals with traces of dissolution, indicating equilibria condition and/or a relatively small change in the physical condition of the system.

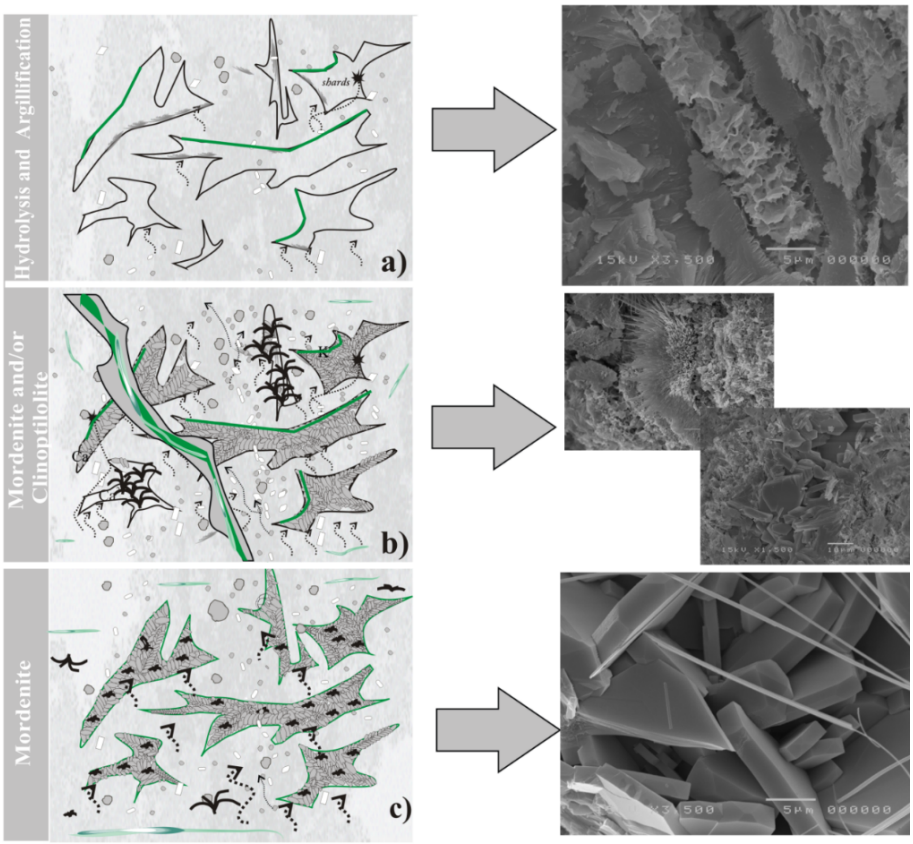

Figure 10. Proposed conceptual model of the zeolitization process (modified by [30]) and supporting textures in the rocks imaged by electron microscopy. Three steps are hypothesized: (**a**) hydration and hydrolysis of the volcanic glass with smectite formation; (**b**) transformation in mordenite and subordinate glauconite development; (**c**) clinoptilolite formation [52].

6. Conclusions

Field observations and analytical investigations on zeolite-bearing epiclastites of Asuni units allow to suggest a mineralogical and genetic model that may have implications for mineral exploration in central Sardinia and paleo-environmental reconstructions as well.

The different types, distribution and abundance of the zeolites can be explained by considering an open hydrologic system, continuously evolving due to water-rock interaction and supply of marine waters after eruption. As result, a different concentration and chemistry of the zeolite minerals occurred at specific levels in the sequences. In particular, we can identify a clinoptilolite enrichment in the lower part of the Asuni Unit, which unlike the higher levels is enriched in mordenite.

The data presented in this study on the Asuni tuffites improves the existing background about the areal distribution of zeolite occurrences in central Sardinia. Considering that this study may contribute to an evaluation of the quality and the reserves of zeolite mineralization, it is aimed at a possible future exploitation and potential use in the Mediterranean area.

Supplementary Materials: The following are available online at http://www.mdpi.com/2075-163X/10/3/268/s1, Figure S1: XRPD patterns of samples from Pranu Pirastru, where the most representative zeolite-bearing unit of the Asuni deposit occurs, with enlargements related to the ranges 5–15°, 20–38° and 42–60°. Abbreviations: Cl, clinoptilolite, Mo, mordenite, Qz, quartz; Fls, feldspar (Fl, fluorite, is an internal standard). Table S1: Composition of oxide (wt %) for selected clinoptilolite crystals by EDS; Table S2: Composition of oxide (wt %) for selected mordenite crystals, obtained by EDS analyses. References [69] are cited in the supplementary materials.

Author Contributions: Conceptualization, A.M.; software, A.M. and M.P.; methodology and formal analysis, A.M.; data curation, A.M. and M.P.; writing—original draft preparation, A.M.; writing—review and editing A.M. and M.P. All authors have read and agreed to the published version of the manuscript.

Funding: This research was granted by the Programma Operativo Nazionale Ricerca Scientifica, Sviluppo, Alta Formazione 2000–2006, funded by the Italian Ministry of Education, University and Research (MIUR).

Acknowledgments: This study is part of the PhD Thesis of A. Mormone at the University of Napoli "Federico II". The authors would like to thank M.R. Ghiara for her useful suggestions. We are grateful to R. de Gennaro for help with SEM and EDS analyses. Two anonymous reviewers are acknowledged for their helpful and constructive comments, which greatly improved the manuscript. The authors also thank the Editors and the editorial staff for handling the manuscript. Emily Sophia Shepherd is thanked for careful English revision of the manuscript.

Conflicts of Interest: The authors declare no conflict of interest.

References

1. Boni, M.; Alt, J.; Balassone, G.; Russo, A. Stratabound ores at the mid-Ordovician unconformity in SW Sardinia: Depositional environment and isotopic characteristics. *IGCP Proj.* **1992**, 67–70.
2. Aversa, G.; Balassone, G.; Boni, M.; Amalfitano, C. The mineralogy of the «calamine» Ores in SW Sardinia (Italy): Preliminary results. *Period. Mineral.* **2002**, *71*, 201–218.
3. Boni, M.; Muchez, P.; Schneider, J. Permo-Mesozoic multiple fluid flow and ore deposits in Sardinia: A comparison with post-Variscan mineralization of Western Europe. *Geol. Soc. Spec. Publ.* **2002**, *204*, 199–211. [CrossRef]
4. Mondillo, N.; Boni, M.; Balassone, G.; Spoleto, S.; Stellato, F.; Marino, A.; Santoro, L.; Spratt, J. Rare earth elements (REE)-Minerals in the Silius fluorite vein system (Sardinia, Italy). *Ore Geol. Rev.* **2016**, *74*, 211–224. [CrossRef]
5. Garbarino, C.; Masi, U.; Padalino, G.; Palomba, M. Geochemical features of the kaolin deposits from Sardinia (Italy) and genetic implications. *Chem. Erde.* **1994**, *54*, 213–233.
6. Cara, S.; Carcangiu, G.; Padalino, G.; Palomba, M.; Tamanini, M. The bentonites in pelotherapy: Thermal properties of clay pastes from Sardinia (Italy). *Appl. Clay Sci.* **2000**, *16*, 125–132. [CrossRef]
7. Palomba, M.; Padalino, G.; Marchi, M. Industrial mineral occurrences related to Cenozoic volcanic rocks of Sardinia (Italy). In Proceedings of the 7th Biennial SGA Meeting, Athens, Greece, 24–28 August 2003; Volume 1, pp. 919–922.
8. Cara, S.; Carcangiu, G.; Massidda, L.; Meloni, P.; Sanna, U.; Tamanini, M. Assessment of pozzolanic potential in lime-water systems of raw and calcined kaolinic clays from the Donnigazza Mine (Sardinia-Italy). *Appl. Clay Sci.* **2006**, *33*, 66–72. [CrossRef]

9. Palomba, M.; Padalino, G.; Marchi, M. Industrial mineral occurrences associated with Cenozoic volcanic rocks of Sardinia (Italy): Geological, mineralogical, geochemical features and genetic implications. *Ore Geol. Rev.* **2006**, *29*, 118–145. [CrossRef]
10. Persico, C.; De Arca, A.; Spada, F. *Le Industrie Estrattive In Sardegna: Analisi Economica E Strutturale*; Osservatorio Economico della Sardegna: Cagliari, Italy, 2007; p. 11.
11. Marcello, A.; Mazzella, A.; Naitza, S.; Pretti, S.; Tocco, S.; Valera, P.; Valera, R. Carta Metallogenica e delle Georisorse della Sardegna in scala 1: 250.000-Metallogenic and Geo-resouces map of Sardinia 1: 250000 scale. 2008. Available online: https://iris.unica.it/handle/11584/94344?mode=full.76#.Xm3FQXIRXIU (accessed on 14 March 2020).
12. Costamagna, L.G.; Cruciani, G.; Franceschelli, M.; Puxeddu, M. A volcano-sedimentary sequence with albitite layers in the Variscan basement of NE Sardinia: A petrographical and geochemical study. *Period. Mineral.* **2012**, *81*, 179–204.
13. Langella, A.; Cappelletti, P.; Cerri, G.; Bish, D.L.; Gennaro, M. de' Distribution of Industrial Minerals in Sardinia (Italy): Clinoptilolite Bearing Rocks of the Logudoro Region. In *Natural Microporous Materials in Environmental Technology*; Springer: Berlin/Heidelberg, Germany, 1999; 528p.
14. Passaglia, E.; Sheppard, R.A. The crystal chemistry of zeolites. *Rev. Mineral. Geochem.* **2001**, *45*, 69–116. [CrossRef]
15. Mercurio, M.; Sarkar, B.; Langella, A. Preface. In *Modified Clay and Zeolite Nanocomposite Materials*; Elsevier: Amsterdam, The Netherlands, 2019.
16. Shen, J.H.; Wang, Y.S.; Lin, J.P.; Wu, S.H.; Horng, J.J. Improving the indoor air quality of respiratory type of medical facility by zeolite filtering. *J. Air Waste Manag. Assoc.* **2014**, *64*, 13–18. [CrossRef] [PubMed]
17. Mažeikien, A.; Valentukevičien, M.; Jankauskas, J. Laboratory study of ammonium ion removal by using zeolite (Clinoptilolite) to treat drinking water. *J. Environ. Eng. Landsc. Manag.* **2010**, *18*, 54–61. [CrossRef]
18. Sharadqah, S.I.; Al-Dwairi, R.A. Control of odorants emissions from poultry manure using jordanian natural zeolites. *Jordan J. Civ. Eng.* **2010**, *4*, 378–388.
19. Yu, C.H.; Huang, C.H.; Tan, C.S. A review of CO_2 capture by absorption and adsorption. *Aerosol Air Qual. Res.* **2012**, *12*, 745–769. [CrossRef]
20. Özen, S.; Göncüoğlu, M.C.; Liguori, B.; De Gennaro, B.; Cappelletti, P.; Gatta, G.D.; Iucolano, F.; Colella, C. A comprehensive evaluation of sedimentary zeolites from Turkey as pozzolanic addition of cement- and lime-based binders. *Constr. Build. Mater.* **2016**, *105*, 46–61. [CrossRef]
21. Ahmed, N.M.; Emira, H.S.; Selim, M.M. Anticorrosive performance of ion-exchange zeolites in alkyd-based paints. *Pigment Resin Technol.* **2011**, *40*, 91–99. [CrossRef]
22. Andronikashvili, T.; Pagava, K.; Kurashvili, T.; Eprikashvili, L. Possibility of Application of Natural Zeolites for Medicinal Purposes. *Bull. Georg. Natl. Acad. Sci.* **2009**, *3*, 158–167.
23. de'Gennaro, M.; Oggiano, G.; Langella, A.; Di Pisa, A. Technological perspectives from volcaniclastic rocks of North Sardinia. *Sci. Tecn. Zeol.* **1995**, 337–345.
24. Ghiara, M.R.; Petti, C.; Franco, E.; Luxoro, S.; Gnazzo, L. Diagenetic clinoptilolite from pyroclastic flows of northern Sardinia. In Proceedings of the 3° Convegno Naz. di Sci. e Tecnol. delle Zeoliti, Ce-traro, Italy, 28–29 September 1995; pp. 349–353.
25. Ghiara, M.R.; Lonis, R.; Petti, C.; Franco, E.; Luxoro, S.; Balassone, G. The zeolitization process of Tertiary orogenic ignimbrites from Sardinia (Italy): Distribution and mining importance. *Period. Mineral.* **1997**, *66*, 211–229.
26. Cappelletti, P.; Cerri, G.; dé Gennaro, M.; Langella, A.; Naitza, S.; Padalino, G.; Rizzo, R.P.M. Natural zeolites from Cenozoic pyroclastic flows of Sardinia (Italy): Evidence of different minerogenetic processes. The Sector of Asuni (Central Sardinia). In *Proceeding of 10th International Symposium on Water-Rock Interaction, WRI-10, Villasimius, Italy, 10–15 June, 2001*; A.A. Balkema: Amsterdam, The Netherlands, 2001; pp. 681–684.
27. Cappelletti, P.; Cerri, G.; de Gennaro, M.; Langella, A.; Naitza, S.; Padalino, G.; Palomba, M.; Rizzo, R. 01-O-02-Natural zeolites mineralization in the Oligocene-Miocene volcano-sedimentary succession of Central Sardinia (Italy). *Stud. Surf. Sci.Catal.* **2001**, *135*, 147.
28. Cerri, G.; Cappelletti, P.; Langella, A.; De'Gennaro, M. Zeolitization of oligo-miocene volcaniclastic rocks from Logudoro (northern Sardinia, Italy). *Contrib. Mineral. Petrol.* **2001**, *140*, 404–421. [CrossRef]
29. Cerri, G.; Oggiano, G. Le epiclastiti zeolitizzate del Logudoro orientale: Un livello guida all'interno della successione vulcano-sedimentaria della Sardegna centrosettentrionale. *Boll.-Soc. Geol. Ital.* **2001**, *121*, 3–10.

30. Mormone, A.; Ghiara, M.R.; Balassone, G.; Piochi, M.; Lonis, R.; Rossi, M. High-silica zeolites in pyroclastic flows from Central Sardinia (Italy): Clues on genetic processes and reserves from a mineralogical study. *Mineral. Petrol.* **2018**, *112*, 767–788. [CrossRef]
31. Naitza, S.; Rizzo, R.; Naitza, S.; Padalino, G.; Palomba, M.; Rizzo, R. Distribution and genesis of zeolite mineralization in Cenozoic pyroclastic flows from Central Sardinia (Italy): Guidelines for mineral exploration Geo resources planning View project Variscan ore deposits in Sardinia View project Distribution and genesis of zeolite mineralization in Cenozoic pyroclastic flows from Central Sardinia (Italy): Guidelines for mineral exploration. In *Mineral Exploration and Sustainable Development*; Millpress: Rotterdam, The Netherlands, 2003; pp. 915–918.
32. de'Gennaro, M.; Langella, A.; Padalino, G.; Palomba, M. Zeolite-bearing mineralization at monte Ossoni (Castelsardo, Northern Sardinia) and at Allai-Samugheo area (central Sardinia) as possible deposits of industrial minerals. In Proceedings of the IV Convegno Nazionale Scienza E Tecnologia Delle Zeoliti, Cernobbio, Italy, September 1998; pp. 57–59.
33. Tilocca, G.; Sistu, G. Il Monte Zuighe (Logudoro, Sardegna nord-occidentale): Osservazioni geologiche e litogeochimiche. *Boll. della Soc. Geol. Ital.* **1994**, *113*, 633–644.
34. Morbidelli, P.; Ghiara, M.R.; Lonis, R.; Sau, A. Zeolitic occurrences from tertiary pyroclastic flows and related epiclastic deposits outcropping in northern sardinia (Italy). *Period. Mineral.* **1999**, *2*, 287–313.
35. Cerri, G.; Mameli, P. Secondary mineral assemblages within epiclastites of western Logudoro, Sardinia, Italy. In *Proceedings of the Rocky Mountain (56th Annual) and Cordilleran (100th Annual) Joint Meeting, (3–5 May 2004)*; Geological Society of America: Boulder, CO, USA, 2004; Volume 36, p. 81.
36. Cappelletti, P.; Langella, A.; Cruciani, G. Crystal-chemistry and synchrotron Rietveld refinement of two different clinoptilolites from volcanoclastites of North-Western Sardinia. *Eur. J. Mineral.* **1999**, *11*, 1051–1060. [CrossRef]
37. Brotzu, P.; Ghiara, M.R.; Cincotti, F.; Lonis, R.; Fercia, M.L.; Sau, A. Distribuzione dei minerali autigeni nei flussi piroclastici dell'Unità di Allai (Sardegna Centro-Meridionale). In Proceedings of the 85° Congresso SIMP, Fluminimaggiore-Antas, Italy, 27–30 September 2006.
38. Hippolyte, J.-C.; Angelier, J.; Roure, F.; Casero, P.; Hyppolite, J.; Angelier, J.; Roure, F.; Geology, P. Piggyback basin development and thrust belt evolution: Structural and palaeostress analyses of Plio-Quaternary basins in the Southern Apennines. *J. Struct. Geol.* **1994**, *16*, 159–174. [CrossRef]
39. Carmignani, L.; Carosi, R.; Di Pisa, A.; Gattiglio, M.; Musumeci, G.; Oggiano, G.; Carlo Pertusati, P. The hercynian chain in Sardinia (Italy). *Geodin. Acta* **1994**, *7*, 31–47. [CrossRef]
40. Beccaluva, L.; Bianchini, G.; Siena, F. *Tertiary-Quaternary Volcanism and Tectono-Magmatic Evolution in Italy*; Crescenti, U., D'Offizi, S., Merlino, S., Sacchi, L., Eds.; Società Geologica Italiana: Florence, Italy, 2004; Volume IGC32, pp. 153–154.
41. Doglioni, C.; Harabaglia, P.; Merlini, S.; Mongelli, F.; Peccerillo, A.; Piromallo, C. Orogens and slabs vs. their direction of subduction. *Earth Sci. Rev.* **1999**, *45*, 167–208. [CrossRef]
42. Speranza, F.; Villa, I.M.; Sagnotti, L.; Florindo, F.; Cosentino, D.; Cipollari, P.; Mattei, M. Age of the Corsica-Sardinia rotation and Liguro-Provençal Basin spreading: New paleomagnetic and Ar/Ar evidence. *Tectonophysics* **2002**, *347*, 231–251. [CrossRef]
43. Cherchi, A.; Mancin, N.; Montadert, L.; Murru, M.; Putzu, M.T.; Schiavinotto, F.; Verrubbi, V. The stratigraphic response to the Oligo-Miocene extension in the western Mediterranean from observations on the Sardinia graben system (Italy). *Bull. Soc. Geol. Fr.* **2008**, *179*, 267–287. [CrossRef]
44. Funedda, A.; Meloni, M.A.; Loi, A. Geology of the Variscan basement of the Laconi-Asuni area (central Sardinia, Italy): The core of a regional antiform refolding a tectonic nappe stack. *J. Maps* **2015**, *11*, 146–156. [CrossRef]
45. Carmignani, L.; MINZON, N.; Pertusati, P.C.; Gattiglio, M. Lineamenti geologici principali del Sarcidano-Barbagia di Belvì. *Mem. della Soc. Geol. Ital.* **1982**, *24*, 119–125.
46. Oggiano, G.; Gaggero, L.; Funedda, A.; Buzzi, L.; Tiepolo, M. Multiple early Paleozoic volcanic events at the northern Gondwana margin: U-Pb age evidence from the Southern Variscan branch (Sardinia, Italy). *Gondwana Res.* **2010**, *17*, 44–58. [CrossRef]
47. Assorgia, A.; Balogh, K.; Lecca, L.; Ibba, A.; Porcu, A.; Secchi, F.; Tilocca, G. Volcanological characters and structural contexst of Oligo-Miocene volcanic succession from Central Sardinia (Italy). *Accad. Naz. Delle Sci. Detta Dei XL* **1995**, *14*, 397–424.

48. Assorgia, A.; Barca, S.; Porcu, A.; Spano, C.; Balogh, K.; Rizzo, R. The Oligocene–Miocene sedimentary and volcanic successions of central Sardinia, Italy. *Rom. J. Stratigr.* **1998**, *78*, 9–23.
49. Ghiara, M.R. Distribution and genesis of zeolites in Tertiary ignimbrites from Sardinia: Evidence of superimposed mineralogenic processes. *Nat. zeolites third Millenn.* **2000**, 177–192.
50. Cappelletti, A.; Ibba, A.; Langella, A.; Naitza, S.; Rizzo, R. Geological and mineralogical study on the great ignimbrite of bosa. first evaluation of zeolite resources for technological applications. In *Proceedings of the 5 Congresso Nazionale Scienza E Tecnologia Delle Zeoliti, 1–5 Octorber 2000*; Società chimica italiana: Roma, Italy, 2000; pp. 229–232.
51. Gottardi, G.; Galli, E. *Natural Zeolites*; Springer: Berlin/Heidelberg, Germany, 1985; Volume 18, 204p.
52. Sheppard, R.A. Distribution and genesis of authigenic silicate minerals in tuffs of Pleistocene Lake Tecopa, Inyo County, California. *US Geol. Surv. Prof. Pap.* **1968**, *597*, 1–38.
53. Whateley, M.K.G.; Querol, X.; Fernández-Turiel, J.L.; Tuncali, E. Zeolites in tertiary coal from the Çayirhan mine, Beypazari, Turkey. *Miner. Depos.* **1996**, *31*, 529–538. [CrossRef]
54. Lecca, L.; Lonis, R.; Luxoro, S.; Melis, E.; Secchi, F.; Brotzu, P. Oligo-Miocene volcanic sequences and rifting stages in Sardinia: A review. *Period. Mineral.* **1997**, *66*, 7–61.
55. Passaglia, E. The crystal chemistry of mordenites. *Contrib. Mineral. Petrol.* **1975**, *50*, 65–77. [CrossRef]
56. Burst, J.F. "Glauconite" Pellets: Their Mineral Nature and Applications to Stratigraphic Interpretations. *Am. Assoc. Pet. Geol. Bull.* **1958**, *42*, 310–327.
57. Burst, J.F. Mineral heterogeneity in "glauconite" pellets. *Am. Mineral. J. Earth Planet. Mater.* **1958**, *43*, 481–497.
58. Hower, J. Some factors concerning the nature and origin of glauconite. *Am. Mineral.* **1961**, *46*, 313–334.
59. Odin, G.S.; Matter, A. De glauconiarum origine. *Sedimentology* **1981**, *28*, 611–641. [CrossRef]
60. Meunier, A.; El Albani, A. The glauconite-Fe-illite-Fe-smectite problem: A critical review. *Terra Nov.* **2007**, *19*, 95–104. [CrossRef]
61. Sheppard, R.A.; Hay, R.L. Formation of zeolites in open hydrologic systems. *Rev. Mineral. Geochem.* **2001**, *45*, 261–275. [CrossRef]
62. Guarino, V.; Fedele, L.; Franciosi, L.; Lonis, R.; Lustrino, M.; Marrazzo, M.; Melluso, L.; Morra, V.; Rocco, I.; Ronga, F. Mineral compositions and magmatic evolution of the calcalkaline rocks of northwestern Sardinia, Italy. *Period. di Mineral.* **2011**, *80*, 517–545.
63. Wirsching, U. Experiments on the hydrothermal formation of calcium zeolites. *Clays Clay Miner.* **1981**, *29*, 171–183. [CrossRef]
64. Sun, S.S.; McDonough, W.F. Chemical and isotopic systematics of oceanic basalts: Implications for mantle composition and processes. *Geol. Soc. Spec. Publ.* **1989**, *29*, 171–183. [CrossRef]
65. Morbidelli, P.; Ghiara, M.R.; Lonis, R.; Petti, C. Quantitative distribution and chemical composition of authigenic minerals in clinoptilolite-bearing ignimbrites from northern Sardinia (Italy): Inferences for minerogenetic models. *Period. Mineral.* **2001**, *70*, 71–97.
66. Mumpton, F.A. Clinoptilolite redefined. *Am. Mineral.* **1960**, *45*, 351–369.
67. Hay, R.L. Phillipsite of saline lakes and soils. *Am. Mineral. J. Earth Planet. Mater.* **1964**, *49*, 1366–1387.
68. Sheppard, R.A.; Gude, A.J., III; Griffin, J.J. Chemical composition and physical properties of phillipsite from the Pacific and Indian Oceans. *Am. Mineral.* **1970**, *55*, 2053–2062.
69. Passaglia, E. The crystal chemistry of chabazites. *Am. Mineral.* **1970**, *55*, 1278–1301.